ELSEVIER

Journal of Alloys and Compounds 421 (2006) 247–251

Journal of ALLOYS AND COMPOUNDS

www.elsevier.com/locate/jallcom

Raman scattering investigation of nanocrystalline δ-TiN_x synthesized by solid-state reaction

Z.H. Ding [a], B. Yao [a,b,*], L.X. Qiu [a], T.Q. Lv [a]

[a] *Department of Physics, Jilin University, Changchun 130023, PR China*

[b] *Key Laboratory of Excited State Process, Chinese Academy of Sciences, Changchun Institute of Optics, Fine Mechanics and Physics, Chinese Academy of Sciences, Changchun 130022, PR China*

Received 2 July 2005; received in revised form 7 November 2005; accepted 10 November 2005
Available online 6 January 2006

Abstract

Micro-Raman scattering has been used to study titanium nitride with rock salt structure (δ-TiN_x) synthesized by mechanical milling of a mixture of metal Ti and hexagonal boron nitride (*h*-BN) powders. The influence of milling time on the Raman spectra of δ-TiN_x was systematically studied. Three peaks at about 215, 315, and 557 cm^{-1}, related to transverse acoustic (TA), longitudinal acoustic (LA), and transverse optical (TO) modes of cubic TiN, respectively, were observed in the Raman spectra of TiN nanocrystals. X-ray diffraction technique was used to study the crystal structures and the average particle sizes. Raman scattering (RS) was employed to investigate the evolution of δ-TiN_x nanocrystalline. The change of lattice constant that caused by the N/Ti ratio is the main reason for the evolution in the Raman spectra of δ-TiN_x nanocrystalline with increasing milling time. The internal stress and grain size play a minor role in Raman spectra of δ-TiN_x nanocrystalline in present study.

Keywords: Raman spectrum; δ-TiN_x; Milling time; Lattice constant

1. Introduction

Raman scattering is a powerful nondestructive technique that gives vibrational information about organic and inorganic. The intensity, frequency, and width of Raman features are strongly dependent on composition, defects, short-range order, crystalline structure, and internal stress in the materials. Therefore, it has been widely used to obtain detailed information about the structural properties of semiconductors, high-T_c superconductors, ceramics, catalysts, carbon based materials, and β-δ nitride materials, including lattice perfection, strain, crystalline, interface, and compositional uniformity [1].

Raman scattering from materials with metallic properties is restricted by prohibitive selection rules, low penetration depth of the incident light (due to high reflectivity), etc. The resulting penetration depth is small ($d = \lambda/4\pi k$, k denoting the absorption coefficient) for these coatings, such as TiN, ZrN, TiCN and TiAlN, but the spectra obtained still arise from a spatial range corresponding to many unit cells [2]. The phonon bands of TiN have been studied extensively by a number of authors [2–6] who have attributed the scattering in the acoustic range to be primarily determined by the vibration of the heavy Ti ions (typically 150–300 cm^{-1}) and in the optic range by vibrations of the lighter N ions (typically 400–650 cm^{-1}).

In this paper we describe the Raman spectra of δ-TiN_x nanocrystalline, which is synthesized during mechanical milling process, focusing on the changes in the spectral center shift and density.

2. Experimental process

The raw materials used in this study were Ti powder of 99% purity and hexagonal BN powder of 99% purity. The mixture with an atomic ratio of BN to Ti of 78:22 was mechanically milled under Ar atmosphere in a high-energy ball-mill machine, using stainless steel balls and vial.

The structure and grain size of the samples were investigated by using X-ray diffractometer (XRD) with Cu Kα radiation, Raman spectrum was recorded in a backscattering geometry with HR800 integrated Raman system (Jobin-Yvon, France), using the 632.8 nm line of a He–Ne gas laser. The Raman radiation was dispersed and detected by a cooled CCD array yielding spectra in the region from 50 to 1200 cm^{-1} at 1 cm^{-1} resolution. The simple was inspected through a microscope (Olympus) and measured on a spot with a diameter of 1 μm. Because of the small sample spot the laser powder was limited to

* Corresponding author.
E-mail address: binyao@mail.jlu.edu.cn (B. Yao).

0925-8388/$ – see front matter © 2005 Elsevier B.V. All rights reserved.
doi:10.1016/j.jallcom.2005.11.017

20 mW. Spectra are presented as intensity (counts) versus Raman shift (cm^{-1} in air).

3. Results and discussions

Fig. 1 shows XRD patterns of the mixtures of Ti and *h*-BN with different milling time. After milling for 50 h, all diffraction peaks of *h*-BN disappeared, as shown in Fig. 1b. A diffuse diffraction peak ranging from about $2\theta = 10–30^\circ$ was observed, indicating that *h*-BN was transformed into amorphous BN (*a*-BN). The weak diffuse diffraction peak about $2\theta = 30–50^\circ$, implying that amorphous alloy may be formed. Raman scattering measurement was performed for the 50 h-milled mixture to identify the amorphous alloy, as shown in Fig. 3a. The spectrum is similar to that of TiN [1,2], the low-frequency scattering below 370 cm^{-1} is caused by acoustical phonons, and the high-frequency scattering around 550 cm^{-1} is due to optical phonons. [5] Implying that the amorphous alloy is Ti–N amorphous alloy. Furthermore, Ti–N amorphous alloy has similar Raman spectrum as crystalline δ-TiN_x.

After 70 h milling, the XRD intensity of the amorphous Ti–N alloy increases (Fig. 1c), implying more amorphous Ti–N alloy is formed. In addition, a weak diffraction peak is observed at $2\theta = 42.1^\circ$, which is almost the same as the position of the strongest diffraction peak (2 0 0) of δ-TiN_x. Raman spectrum of the 70 h-milled mixture was shown in Fig. 3b. Therefore, it is believed that δ-TiN_x began to form upon milling for 70 h. It is due to crystallization of the amorphous Ti–N alloy driven by the local temperature and local pressure induced by collision of steel balls. [7] With increasing milling time, the XRD peaks intensity of δ-TiN_x increase and all peaks' FWHM become narrower (Fig. 1d), implying more Ti has reacted with N to form δ-TiN_x. Meanwhile, the grain size of δ-TiN_x increases as milling time rises, as shown in Fig. 2. The grain size was calculated by Scherer formula: $D = 0.89\lambda/B\cos\theta$, where λ is the X-ray wavelength, B, full width of half maximum (FWHM) and θ, the Bragg diffraction angle.

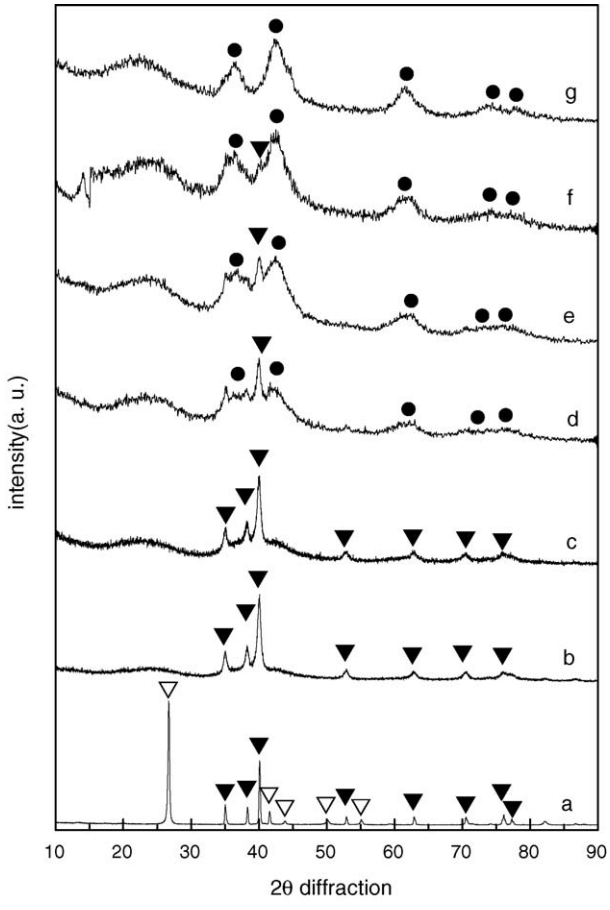

Fig. 1. XRD patterns of the mixture of Ti and h-BN powder milled for (a) 0 h; (b) 50 h; (c) 70 h; (d) 100 h; (e) 120 h; (f) 140 h; and (g) 160 h, respectively. ▽, *h*-BN; ▼, Ti; ●, δ-TiN_x.

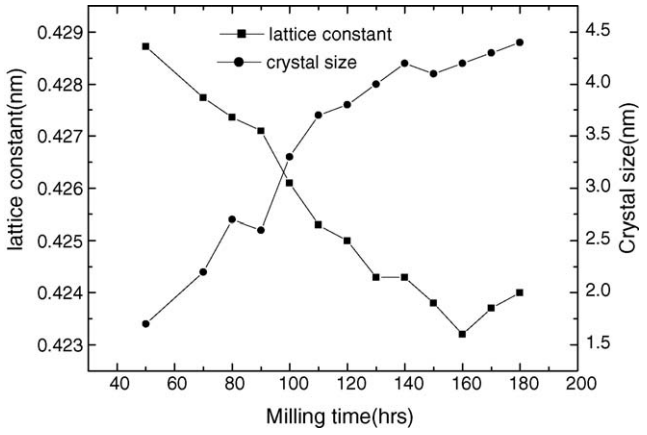

Fig. 2. Grain size and lattice constant of δ-TiN_x for different milling time.

It is also found from the XRD results that there always exists a diffraction peak of the amorphous Ti–N alloy for samples prepared at milling times less than 140 h, indicating Ti does not react completely with *a*-BN. Upon 150 h, the diffraction peaks of both Ti and amorphous Ti–N alloy disappeared completely, the XRD pattern consists of diffraction peaks of *a*-BN and δ-TiN_x, as shown in Fig. 1e. It indicates that all Ti react with N in the *a*-BN to form δ-TiN_x. Lattice constant of δ-TiN_x produced at different milling times was calculated, and revealed in Fig. 2. The lattice constant decreases monotonic up to 160 h milling.

In order to better understanding the changes in the Raman spectrum of δ-TiN_x nanocrystallines with milling time, the Raman spectra at the range of 100–800 cm^{-1} were fitted using the Gaussian and Lorentzian profiles. Two broad and weak peaks at 150–350 cm^{-1} and 450–700 cm^{-1} can be observed, as shown in Fig. 3a and b. The typical deconvolution result of Raman spectrum for 180 h milled sample is shown in Fig. 4. The spectrum can be fitted well with three Lorentzian peaks at about 215, 315, and 557 cm^{-1}. As shown in Figs. 3 and 4, The Raman lines at 210–230, 310–330, and 540–560 cm^{-1} can be assigned as transverse acoustic (TA), longitudinal acoustic (LA) and transverse optical (TO) modes of the cubic TiN nanocrystallines, respectively [2].

It is well known that in a perfect crystal with fcc structure, every ion is at a site of inversion symmetry and consequently first-order Raman scattering is forbidden. However, mechanical milled coatings are known to contain many microscopic defects, i.e. both heavy metal Ti ion and also lighter nitrogen

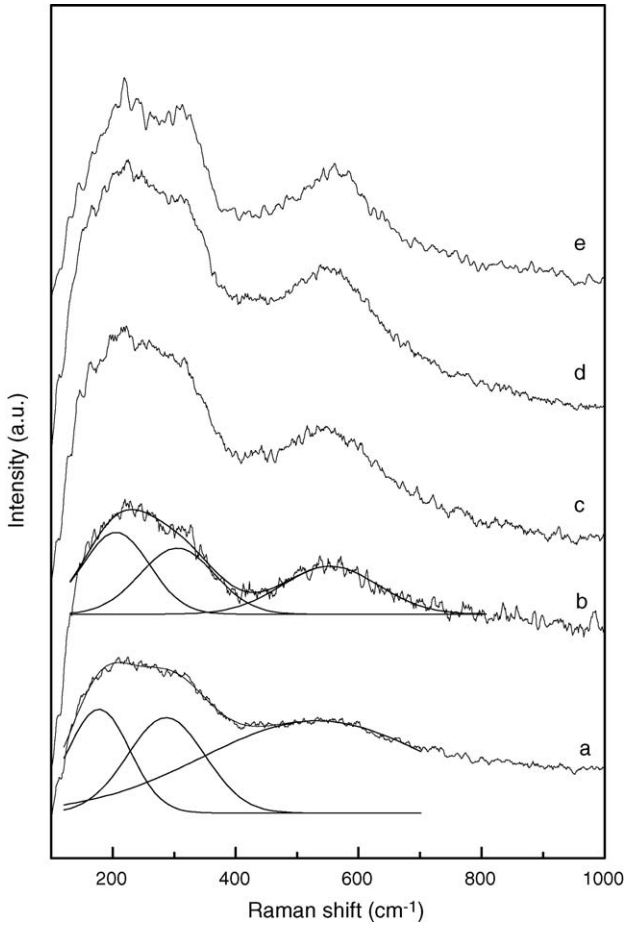

Fig. 3. Raman spectra of mixture milled for various milling times.

ion site vacancies are present. These defects reduce the effective symmetry and certain atomic displacements of neighboring atoms have non-zero first-order polarizability derivatives. The first-order Raman spectrum of a perturbed crystal reflects the density of states for those atomic displacements rendered Raman active by the presence of the impurity/defect [8].

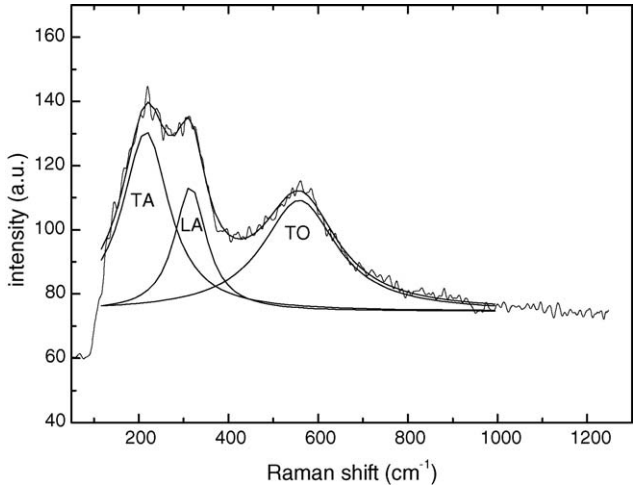

Fig. 4. Typical deconvolution result of Raman spectrum for the sample milled for 180 h.

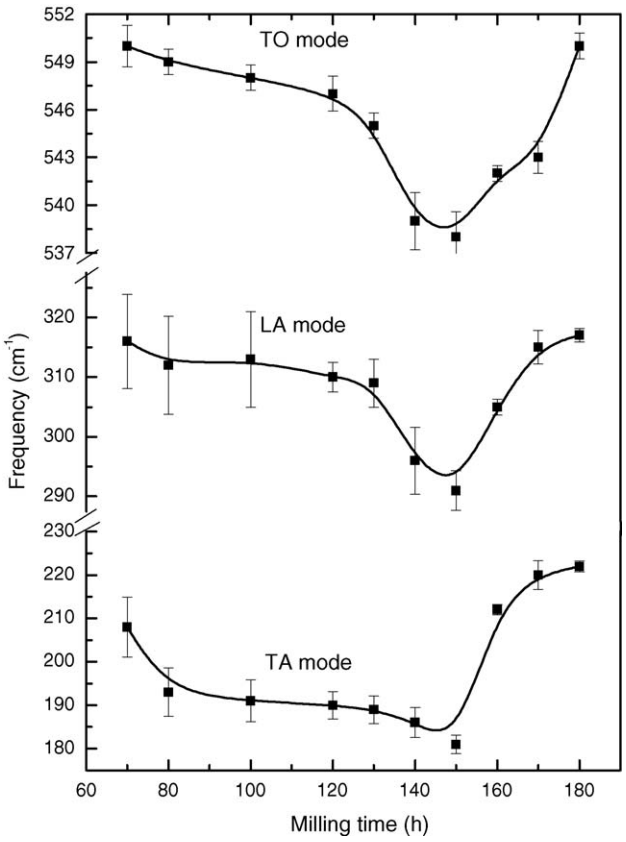

Fig. 5. Dependence of the frequency of TA, LA, and TO Raman peaks on the milling time.

The frequency changes of TA, LA, and TO mode with variation of milling time are shown in Fig. 5. It is worth noting that the three peaks shift gradually to lower frequency with increasing milling time, reaching a minimum when milling time over 150 h, then shift to high frequency. Fig. 6 shows the influence of milling time on the FHMW of TA, LA, and TO mode Raman peaks. The FWHM of three Raman active mode decrease gradually before milled 130 h, then increase slightly when milling 130–160 h. By comparing Fig. 5 with Fig. 2, it is clearly observed that the

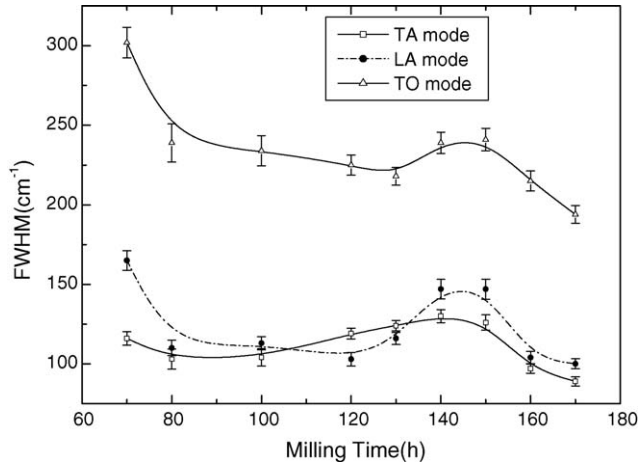

Fig. 6. Dependence of FHWM of TA, LA, and TO Raman peaks on the milling time.

Table 1
Raman shift frequency and FWHM changes of δ-TiN_x after annealing at 350 °C for 2 h in high vacuum (10^{-3} Pa)

Samples	TA mode (cm^{-1})		LA mode (cm^{-1})		TO mode (cm^{-1})	
	Frequency	FWHM	Frequency	FWHM	Frequency	FWHM
140 h	200 ± 1.2	132 ± 3.9	305 ± 1.8	144 ± 5.8	553 ± 1.4	241 ± 7.1
Annealed	228 ± 0.9	84 ± 3.5	312 ± 1.3	99 ± 4.3	572 ± 1.5	224 ± 9.4
150 h	193 ± 1.4	126 ± 4.8	296 ± 2.1	147 ± 6.3	557 ± 1.4	241 ± 7.1
Annealed	229 ± 0.9	80 ± 3.3	313 ± 1.3	96 ± 4.2	577 ± 1.2	224 ± 6.9
160 h	210 ± 1.0	92 ± 3.4	301 ± 1.4	105 ± 4.6	551 ± 1.6	226 ± 8.5
Annealed	227 ± 1.3	89 ± 4.9	316 ± 2.0	97 ± 6.6	577 ± 1.2	224 ± 6.9

variation trend in the position of the three peaks fit well with the lattice constant change. A decrease in the lattice constant is expected to result in a shift of the peak to lower frequency.

Generally, the main factors that are responsible for the shift of the Raman spectra are composition, grain size, defects, and internal stress in the sample powder. As discussed in ours another article [9], N atoms in the *a*-BN incorporate into nanocrystalline Ti with a large amount of defects induced during milling process to form amorphous Ti–N alloy. When the phase diagram of N–Ti is considered, the solubility of N in Ti at room temperature is very low, and when N content in amorphous alloy exceeds some critical value, which should be above 30 at.% [10], amorphous Ti–N crystallizes to δ-TiN_x driven by the local temperature and local pressure [11]. With extending milling time, N atoms continue dissolve into nanocrystalline Ti to form amorphous Ti–N alloy; on the other hand, N atoms also incorporate into amorphous Ti–N and δ-TiN_x, leading to increment of N content of δ-TiN_x. Excessive Ti occupies N positions in Ti-rich δ-TiN_x. Since atomic radium of N is less than that of Ti, the Ti-rich δ-TiN_x has larger lattice constant, and the lattice constant decreases with increasing N content. Therefore, the decrease of the lattice constant of δ-TiN_x in Fig. 2 is attributed to increment of N content in δ-TiN_x with increasing milling time.

When milling time upon 150 h, Ti reacts completely with *a*-BN. Continual milling may cause more N atom diffuse into the δ-TiN_x to form N-rich δ-TiN_x nanocrystalline supersaturated solutions. The excess N atoms in the N-rich δ-TiN_x may exist in a form of interstitial atoms, leading to increment of lattice constant of δ-TiN_x. We deduced the variation in lattice parameter is in accordance with the variation of N content in δ-TiN_x, after consulting our result with Joint Committee Powder Diffraction Standard (JCPDS) card No. 87-0626, 71-0299, and 87-0628. As shown in Fig. 7, the lattice constant of TiN_x increase when N content increase from 43.2 to 50 at.%. We estimate N content in δ-TiN_x no less then 50% atom ratio after 180 h milled. From Fig. 5, it is easy to find that the centers of Raman peaks slightly shift to high frequency after 150 h milling. We deduce it is also caused by the increase in lattice constant of δ-TiN_x.

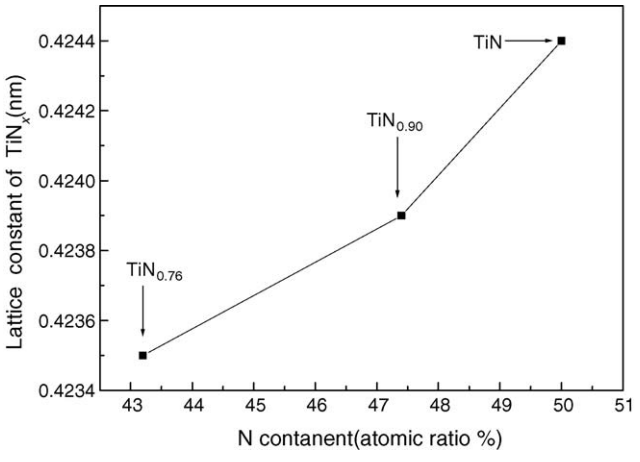

Fig. 7. Effect of N content in TiN_x on the lattice constant.

The grain size increases from 1.7 to 4.4 nm in Fig. 2. It may cause the decrease of the FWHM of Raman spectra in Fig. 6. The Raman peaks width changes with the increasing grain size may be due to the bigger grain size resulting in good crystallinity [12]. The internal stress in nanocrystalline δ-TiN_x also affects the frequency and FWHM of Raman spectra. In order to remove the internal stresses, the samples were annealed at 350 °C for 2 h at high vacuum. As shown in Table 1, TA, LA, and TO modes Raman shifts frequency are all shift to higher frequency and FWHM become narrower after annealing. It is believe that before 120 h, the grain size is not more then 4 nm, so the internal stress could not affect the frequency and FWHM of Raman spectra obviously. Upon 130 h milled time, the crystal increases to more than 4 nm, so the internal stress affects the frequency and FWHM of Raman spectra obviously.

4. Conclusions

Nanocrystalline δ-TiN_x was prepared by mechanical milling of the mixture of Ti and BN. δ-TiN_x is formed by diffuse reaction between Ti and a-BN and phase transition during milling process in the present experiment.

The milling time influenced on the frequency and the FWHM of TA, LA, and TO mode Raman peaks of δ-TiN_x. The three peaks shift gradually to lower frequency with increasing milling time, reaching a minimum at the milling time over 150 h, then shift gradually to high frequency. The decrease of the lattice constant of δ-TiN_x attributed to increment of N content in δ-TiN_x with increasing milling time may responsible for the Raman shift. The FWHM of the three Raman spectra decreases with the increase in grain size due to the increase in crystallinity. The internal stress that generated during ball milling process also influenced the Raman frequency and linewidth of the three vibrational modes.

Acknowledgement

We would like to appreciate financial support of national natural science foundation (granted No: 50472003) of People's Republic of China.

References

[1] Y.H. Cheng, B.K. Tay, S.P. Lau, H. Kupfer, F. Richer, J. Appl. Phys. 92 (4) (2002) 1845.
[2] C.P. Constable, J. Yarwood, W.-D. Münz, Surf. Coat. Tech. 116–119 (1999) 155–159.
[3] C.C. Chen, N.T. Liang, W.S. Tse, I.Y. Chen, J.G. Duh, Chin. J. Phys. 32 (2) (1994) 205.
[4] W. Spengler, R. Kaiser, Solid State Commun. 18 (1976) 881.
[5] W. Spengler, R. Kaiser, A.N. Christensen, G. Müller-Vogt, Phys. Rev. B 17 (3) (1978) 1095.
[6] W. Spengler, R. Kaiser, H. Bilz, Solid State Commun. 17 (1975) 19.
[7] B. Yao, S.E. Liu, L. Liu, L. Si, W.H. Su, Y. Li, J. Appl. Phys. 90 (3) (2001) 1650.
[8] G.P. Montgomery Jr., M.V. Klein, B.N. Ganguly, R.F. Wood, Phys. Rev. B 6 (10) (1972) 4047.
[9] Z.H. Ding, B. Yao, L.X. Qiu, S.Z. Bai, X.Y. Guo, Y.F. Xue, W.R. Wang, X.D. Zhou, W.H. Su, J. Alloy Compd. 391 (2005) 77.
[10] J.Q. Yu, W.Z. Yi, B.D. Chen, H.J. Chen, Phase Diagram of Binary alloys, Science and Technology Press of Shanghai, 1987, p. 479.
[11] B. Yao, L. Liu, S.E. Liu, B.Z. Ding, W.H. Su, Y. Li, J. Non-Cryst. Solids 277 (2000) 91.
[12] Z. Iqbal, S. Veprek, J. Phys. C: Solid State Phys. 15 (1982) 377.